MODELLING PARTICLE TRANSPORT IN ANISOTROPIC TURBULENT FLOW

Ali Rashaida
Department of Mechanical Engineering, University of Saskatchewan
Saskatoon, Saskatchewan, S7N 4A5, Canada

Donald J. Bergstrom
Department of Mechanical Engineering, University of Saskatchewan
Saskatoon, Saskatchewan, S7N 4A5, Canada

ABSTRACT

Many turbulent flows of practical interest involve solid walls which introduce significant anisotropy into the flow structure. This paper investigates the use of the Eddy Interaction Model to predict the transport of heavy particles in homogeneous shear flow. Most previous work with the EIM has focused on isotropic turbulence. In this case, we consider particle transport in a flow which involves a single mean velocity gradient, and the associated anisotropy of the Reynolds stress components. The EIM results are generally in close agreement with the dispersion rates obtained in the LES study of Yeh and Lei (1991). The particle fluctuating velocity characteristics are similar to those obtained in the DNS study of Taulbee et al. (1997) for the same strain rate.

INTRODUCTION

Particle transport is encountered in a wide range of engineering flows in both industrial and environmental applications. When the flow can be characterised as a turbulent boundary layer, the flow structure is profoundly affected by the presence of the wall. The mean and fluctuating velocity fields of the fluid phase are highly anisotropic, which then affects the particle transport.

A popular computational model for particle transport is the so called Eddy Interaction Model (EIM). It represents a Lagrangian approach which integrates the particle equation of motion to determine the trajectories of an ensemble of particles, which are then averaged to produce the statistics describing the motion of the particle phase. The EIM reconstructs the instantaneous flow field in terms of a sequence of eddy motions in which and through which the particle is convected. The instantaneous fluid velocity fluctuation is modelled stochastically based on the characteristic scales of the local turbulence field. In an engineering study, the turbulence characteristics would most often be provided by a solution for the mean transport equations in an Eulerian framework using some time-average turbulence model closure.

Much of the development and assessment of EIM performance has considered quasi-isotropic flow, such as that created downstream of a mesh grid mounted in a wind tunnel. In order to be useful for the wall-bounded flows encountered in engineering practice, the performance of the EIM in anisotropic flow needs to be evaluated. The objective of the present study is to test the performance of a specific EIM in predicting the transport of heavy particles in homogeneous turbulent shear flow, where the mean velocity gradient results in significant anisotropy among the normal Reynolds stress components, and a non-zero shear stress. Homogeneous shear flow has been widely investigated using both experiments, e.g. Harris et al. (1977) and Tavoularis and Corrsin (1981), and more recently direct numerical simulation (DNS), e.g. Rogers and Moin (1987). It is relatively well understood, and as such is an appropriate test case. It resembles near-wall flow in so far as it exhibits a mean velocity gradient and Reynolds stress anisotropy. However, unlike near-wall turbulent flow, the mean velocity gradient and associated anisotropy of the turbulence do not change in the transverse direction. As such, homogeneous shear flow captures some but not all of the characteristics of a turbulent boundary layer. We will use it as a first step for investigating the performance of EIM in anisotropic turbulent flow.

To the authors' knowledge no experimental data exists for particle transport in homogeneous shear flow. In order to evaluate the performance of the EIM, we will compare our results to two sets of "particle experiments" which have been performed numerically. The particle dispersion rates predicted by the EIM will be compared to those obtained

by Yeh and Lei (1991) using a Large Eddy Simulation (LES) to reproduce the instantaneous velocity field. The fluctuating particle velocity characteristics will be compared to those obtained by Taulbee et al. (1997) using DNS to generate the flow field. The results obtained using the EIM for particle transport in homogeneous shear flow will also be contrasted with the results of previous studies which considered homogeneous isotropic turbulence (HIST).

EDDY INTERACTION MODELS

The eddy interaction model represents one type of Lagrangian method developed for calculating particle transport. As mentioned above, in the EIM the equation of motion for the particle is integrated to determine the particle trajectory. The particle statistics are then generated by ensemble averaging a sufficiently large number of particle trajectories. In the particle equation of motion, the fluid forces depend on the instantaneous flow properties, which for turbulent flow have some random or incoherent component. In this sense, the EIM can be viewed as implementing a random walk using a set of representative eddies which are reconstructed from the flow field based on the characteristic length and time scales of the local turbulence field. One of the advantages of the EIM is that it is computationally efficient, since the eddy properties are assumed to be constant over the life-time of the eddy. This partly accounts for the fact that it is the particle model used by most CFD codes. A comprehensive description of particle dispersion in gas flows including a discussion of simulation methods is given in the review by Stock (1996).

In our study, we consider the transport of solid particles in a Newtonian fluid, such as air or water. The particles are assumed to be spherical in shape, and much heavier than the fluid. Furthermore, we consider flows where the particle loading is light, so that the particles do not interact with each other, and any modification of the flow structure (mean or turbulent) by the particles is negligible. We adopt the specific form of the EIM developed by Graham and coworkers, see Graham (1996a, 1996b) and Graham and James (1996).

If we only include the viscous drag force and gravitational body force on the particle, then the equation of motion becomes:

$$\frac{d\vec{u}_p}{dt} = \frac{1}{\tau_r}\left(\vec{u}_f(t) - \vec{u}_p(t)\right) + \vec{g} \qquad (1)$$

where $\vec{u}_f$ and $\vec{u}_p$ are the fluid and particle velocities, respectively, and τ_r is the particle relaxation time given by

$$\tau_r = \frac{4\rho_p d_p}{3\rho_f C_D u_r} \qquad (2)$$

Here ρ_f and ρ_p are the fluid and particle densities, respectively, d_p is the particle diameter, C_D is the drag coefficient and u_r is the magnitude of the relative velocity between the particle and fluid. The equation of motion for the particle describes a nonlinear process in so far as the local drag depends on the fluid velocity which is determined by the trajectory of the particle. Following Graham (1996a), if we assume the local fluid velocity to be uniform, then the particle equation of motion can integrated to obtain analytical expressions for the particle velocity and location at the next time step:

$$\vec{u}_p(t+\delta t) = \vec{u}_f - \left(\vec{u}_f - \vec{u}_p(t)\right)e^{-\delta t/\tau_r} + \vec{g}\tau_r\left(1 - e^{-\delta t/\tau_r}\right) \qquad (3)$$

$$\vec{X}_p(t+\delta t) = \vec{X}_p(t) - \left(\vec{u}_f - \vec{u}_p(t)\right)\tau_r\left(1 - e^{-\delta t/\tau_r}\right) - \vec{g}\,\tau_r^2\left(1 - e^{\delta t/\tau_r} - \delta t/\tau_r\right) + \vec{u}_f\delta t \qquad (4)$$

The equations above are used in the EIM to calculate the trajectory of a particle through a reconstruction of the fluid velocity field in the following manner. The instantaneous fluid velocity field is decomposed into a mean and a fluctuating component. The fluctuating component along the particle trajectory is represented by a sequence of eddies, each characterised by a single length, velocity and time scale. The scales are chosen so that the eddies represent the most energetic eddies, since these will have the greatest effect on the particle motion. The velocity scale is selected randomly from a Gaussian distribution with its mean and variance based on the statistical measures of the local turbulence field, so that the eddy reconstruction represents a stochastic process. Within each eddy, for the lifetime of the eddy, the velocity field is uniform and equal to the sum of the mean and fluctuating components.

At the start of a typical integration step, the particle is imagined to be located at the center of an eddy. Over time, the fluid point representing the center of the eddy and the particle are convected forward along two distinct and different trajectories. The association of the particle with a given eddy will cease when one of two events occurs: 1) the eddy lifetime has expired, or 2) the particle trajectory has taken the particle outside the physical domain of the current eddy. Thus, the fluid particle interaction time is set equal to the minimum of the eddy lifetime and the eddy crossing time. If L_e is the eddy length and the effect of gravity is negligible, then the crossing time can be calculated as follows based on the expression for the particle velocity given above:

$$t_e = -\tau_r \log_e\left(1 - (L_e / u_r\tau_r)\right) \quad (5)$$

To maximise computational efficiency, the integration time step would be set equal to the fluid particle interaction time.

In order to obtain agreement with experimental and simulation data, careful attention is given to determining the various time and length scales used by the model. In summarising the specific model formulation adopted by Graham (1996a) below, we will discuss the major features in the context of the particle dispersion characteristics they seek to reproduce. Since practical applications are ultimately interested in the transport of large groups of particles, it is natural to use dispersion rates to describe this behaviour. The first effect to be considered is the *crossing trajectories* effect, which is used to describe the observation that the presence of a drift velocity causes the particle dispersion to be reduced. This behaviour is often explaining by noting that the drift velocity causes the particles to move more quickly through the turbulent eddies, so that they are less effective at collectively dispersing the particles. The crossing trajectories effect is achieved by correctly specifying the fluid particle interaction time, which relates to the choice of eddy time and length scales. Graham and James (1996) indicate that in order to ensure the correct long-time dispersion of fluid and heavy particles settling under gravity, the eddy length scale is specified as twice the Eulerian longitudinal length scale and the eddy time scale as twice the Lagrangian integral time scale. For flows with gravity, it may be necessary to include the effect of gravity on the eddy crossing time.

The second effect, known as the *inertia effect*, refers to the fact that when gravity can be neglected, heavy particles are observed to disperse more rapidly than fluid particles. Graham (1996b) indicates that this effect can be achieved by allowing the fluid particle interaction time to be greater than the eddy lifetime, depending on the local turbulence structure.

The third effect is the *continuity effect*, which describes the fact that in HIST, the longitudinal dispersion coefficient for heavy particles is expected to be twice that in the lateral direction. This is explained by differences in the longitudinal and lateral spatial autocorrelation functions due to the constraint of continuity. This effect is implemented by using different interaction times in different coordinate directions.

Complete details of the specific rationale for determining the interaction times used in the EIM are given in Graham (1996a). We have implemented his model and tested it to verify that our code reproduces the important features of HIST identified in his paper. We have also used it to successfully predict the dispersion rates measured by Snyder and Lumley (1977) for particle transport in grid generated turbulence. Our model formulation and dispersion results are documented in the thesis of Rashaida (1998).

HOMOGENEOUS SHEAR FLOW

As a test case for EIM applications intended for wall bounded flows, we consider particle transport in homogeneous shear flow. Homogeneous shear flow is a simple turbulent flow characterised by a single non-zero strain rate, in this case the shear component $S = dU_1/dx_2$ where U_1 is the streamwise velocity component, and x_2 is the transverse coordinate direction. Although the flow is described as homogeneous, in experimental and DNS simulations there is typically observed to be some streamwise evolution toward an equilibrium state. In the final stages of evolution, Tavoularis (1989) suggests that the anisotropy of the Reynolds stress components and the Taylor microscale are approximately constant. In regard to particle transport, it is the presence of the mean transverse shear and the associated anisotropy of the Reynolds stress components that suggests the usefulness of this flow in capturing some of the effects present in near-wall turbulent flows.

For the purpose of generating the Eulerian flow field, we use a second-moment closure following Lee and Chung (1995). The specific focus of their study was the equilibrium state and associated stability/instability of the model equations based on different pressure-strain correlation's. For our purposes, the linear pressure-strain model of Launder et al. (1975) is adequate to capture the anisotropy of the flow. Using the formulation of Lee and Chung (1995) for the special case of homogeneous shear flow, the transport equations which govern the flow development reduce to the following five ordinary differential equations:

$$\frac{dk^*}{dt^*} = -\left(2b_{12} + \frac{\varepsilon}{Sk}\right)k^* \quad (6)$$

$$\frac{d}{dt^*}\left(\frac{\varepsilon}{Sk}\right) = 2(1 - C_{\varepsilon 1})\left(\frac{\varepsilon}{Sk}\right)b_{12} + (1 - C_{\varepsilon 2})\left(\frac{\varepsilon}{Sk}\right)^2 \quad (7)$$

$$\frac{db_{11}}{dt^*} = \beta_0\left(\frac{\varepsilon}{Sk}\right)b_{11} + \beta_1 b_{12}b_{11} + \beta_2 b_{12}b_{22} + \beta_3 b_{12} \quad (8)$$

$$\frac{db_{22}}{dt^*} = \beta_0\left(\frac{\varepsilon}{Sk}\right)b_{22} + \beta_4 b_{12}b_{11} + \beta_5 b_{12}b_{22} + \beta_6 b_{12} \quad (9)$$

$$\frac{db_{12}}{dt^*} = \beta_0\left(\frac{\varepsilon}{Sk}\right)b_{12} + \beta_7 b_{12}^2 + \beta_8 b_{11}^2 + \beta_9 b_{22}^2$$

$$+ \beta_{10} b_{11} b_{22} + \beta_{11} b_{11} + \beta_{12} b_{22} + \beta_{13} \qquad (10)$$

where β_0=-1, and the values of all other non-zero β_i's are given in Table 1.

TABLE 1. MODEL COEFFICIENTS

β_i	Value	β_i	Value
β_1	2.00	β_7	2.00
β_3	-0.388	β_{11}	0.109
β_5	2.00	β_{12}	-0.236
β_6	0.303	β_{13}	-0.133

In the equations above, the anisotropy tensor is defined as

$$b_{ij} = \langle u_i u_j \rangle / k - (2/3)\delta_{ij} \qquad (11)$$

based on the Reynolds stress $\langle u_i u_j \rangle$. The turbulence kinetic energy k is normalised by its initial value, $k^*=k/k_0$ and the time t is normalised by the reciprocal of the strain rate S, $t^*=S\,t$. The equation for the (normalised) turbulence time scale, Sk/ε, is obtained by combining the transport equations for k and ε.

The model equations were integrated forward in time (corresponding to streamwise displacement in the physical facility) using a fourth order Runge-Kutta method to predict the development of the Reynolds stress field for the flow studied experimentally by Harris et al. (1977). Their wind tunnel study considered a mean velocity of *12.4 m/sec* and a shear rate of S = *44 sec*$^{-1}$. (According to a corrigendum, Harris et al. (1978), the actual shear rate was in fact slightly larger, *48 sec*$^{-1}$.) The predicted values for the components of the anisotropy tensor at the end of the test section using a shear rate of S = *44 sec*$^{-1}$ are compared to the values given by Harris et al. (1977) in Table 2. While not in exact agreement, the predicted values are at least as good as those obtained by the LES field simulated by Yeh and Lei (1991).

TABLE 2. ANISOTROPY TENSOR

Component	Predicted	HGC (1977)
b_{11}	0.382	0.337
b_{22}	-0.282	-0.268
b_{33}	-0.100	-0.068
b_{12}	-0.290	-0.297

PARTICLE TRANSPORT IN SHEAR FLOW

Dispersion Rates

The EIM described above and previously tested in HIST was used to simulate particle transport in a shear flow similar to that studied by Harris et al. (1977). The predictions for the dispersion rates are compared to those obtained by Yeh and Lei (1991) using LES to generate the instantaneous flow field. Their study considered air and spherical solid particles of different sizes with a density of ρ_p = *2420 kg/m*^{3} which is typical of glass. The body force was taken to act in a direction transverse to the mean flow, i.e. $g_1 = g_3 = 0$, and g_2 = *-9.81 m/sec*^{2}. The particle equation of motion was the same as that given in equation (1), with the viscous drag term expressed by the following relation:

$$C_D = \frac{24}{\mathrm{Re}_p}, \qquad \mathrm{Re}_p < 1$$
$$C_D = \frac{24}{\mathrm{Re}_p}\left(1 + 0.15\,\mathrm{Re}_p^{0.687}\right), \quad 1 < \mathrm{Re}_p < 1000 \qquad (12)$$

Their dispersion calculations were based on ensembles of 2001 particles.

In our case, the EIM was implemented based on an Eulerian prediction for the Reynolds stress components using the equations described above. The calculated dispersion rates were typically based on ensembles of 6000 particles, which was sufficient to obtain converged particle statistics. One of the differences between HIST and homogeneous shear flow is the non-zero shear stress correlation $\langle u_1 u_2 \rangle$ which arises due to the mean shear. Following the approach of Kennedy and Kollmann (1993), we attempted to reconstruct the instantaneous velocity field in a manner which preserved the correct shear correlation between the streamwise and transverse velocity components, u_1' and u_2'. First, the Reynolds stress tensor was transformed into the principal axes system for which all shear stress components are zero. Within this reference frame, the "random" velocity fluctuation in each direction was determined by sampling a Gaussian distribution with a variance given by the normal Reynolds stress component. Finally, the velocity fluctuations were transformed back into the original coordinate frame, thus ensuring the correct correlation between the components. The effect of this procedure was found to be relatively small for the dispersion times considered. For example, in the case of a *80 μm* particle, including the shear correlation reduced the transverse dispersion rate by less than 4 percent. The effect of including the shear stress was almost negligible except very near the end of the test section. This result is in agreement with the conclusions of Kennedy and Kollmann

(1993) for the case of particle dispersion in a round turbulent jet.

The discussion of the dispersion rates predicted for the particles will first consider the case of zero drift velocity. Excluding the influence of gravity enables us to investigate the effect of the inertia of the particle on the dispersion rates. In our case, by increasing the particle diameter, the particle inertia (and Stokes) number is increased. Figure 1a and 1b plot the dispersion rates in the streamwise and transverse coordinate directions for a particle diameter of *57 μm* with zero drift velocity. In general, the agreement between the EIM and LES results is quite good. The anisotropy of the flow is observed to strongly influence the dispersion rates, so that the dispersion in the streamwise direction is much greater than that in the transverse direction. Unlike the case of HIST, the dispersion rate is observed to decrease as the particle size (and inertia) increases. This effect is much more prominent for the streamwise than the transverse direction. For d_p = 57 *μm*, Yeh and Lei (1991) found the fluid point and particle trajectory to be almost identical. They attributed the large streamwise effect to the inability of particles with larger inertia to follow the streamwise growth of turbulence kinetic energy in the shear flow.

Figure 2 illustrates the effect of a finite drift velocity on the transverse dispersion rate for the same size particle. Consistent with the crossing trajectories effect in HIST, the presence of a drift velocity is to reduce the dispersion rate. In this case the effect is larger for transverse than for the streamwise direction (not shown), possibly due to the fact that the streamwise component is more strongly affected by the mean shear strain.

Particle Velocity Statistics

As a second test of the EIM, the predictions for the particle velocity statistics in a shear flow are compared to those obtained by Taulbee et al. (1997). They integrated the particle equation of motion using the velocity field generated by a DNS. The components of the anisotropy tensor for the fluid and particle are compared in Table 3 for the case of a *46 μm* diameter particle with a relaxation time of $\tau_r = 0.016$. Both the EIM and DNS results are consistent in terms of comparisons between fluid and particle properties. Part of the difference in magnitudes is due to the different turbulence time scales of each simulation. Both studies indicate that the streamwise velocity fluctuation of the particle is greater than that of the fluid, which is consistent with the theoretical results, e.g. Liljegren (1993).

CONCLUSIONS

The EIM of Graham (1996a), primarily developed for HIST, has been used to predict particle transport in homogeneous shear flow. The dispersion rates and particle statistics obtained using the EIM are generally in good agreement with the results of particle studies using LES and DNS. The results do not appear to be especially sensitive to the shear correlation, although this may become more important for long-time dispersion rates. The results suggest that the EIM can be implemented in flows with significant flow anisotropy.

TABLE 3. PARTICLE STATISTICS

	EIM	Taulbee et al. (1997)
Sk/ε	12.2	4.82
b_{11}	0.202	0.361
b_{22}	-0.147	-0.291
b_{33}	-0.142	-0.324
b_{11}^p	0.640	0.630
b_{22}^p	-0.300	-0.417
b_{33}^p	-0.290	-0.414
u_1^p / u_1^f	1.18	1.02
u_2^p / u_2^f	0.37	0.739
k_p / k	0.68	0.82

REFERENCES

Graham, D.I., 1996a, "An Improved Eddy Interaction Model for Numerical Simulation of Turbulent Particle Dispersion," *ASME Journal of Fluids Engineering*, Vol. 118, pp. 819-823.

Graham, D.I., 1996b, "On the Inertia Effect in Eddy Interaction Models," *Int. J. Multiphase Flow*, Vol. 22, pp. 177-184.

Graham, D.I. and James, P.W., 1996, "Turbulent Dispersion of Particles Using Eddy Interaction Models," *Int. J. Multiphase Flow*, Vol. 22, pp. 157-175.

Harris, V.G., Graham, J.A.H., and Corrsin, S., 1977, "Further Experiments in Nearly Homogeneous Turbulent Shear Flow," *J. Fluid Mechanics*, Vol. 81, pp. 657-687.

Kennedy, I.M. and Kollmann, W., 1993, "Role of Turbulent Shear Stresses in Particle Dispersion," *AIAA Journal*, Vol. 31, pp. 1959-1960.

Launder, B.E., Reece, G.J., and Rodi, W., 1975, "Progress in the Development of a Reynolds Stress Closure," *J. Fluid Mechanics*, Vol. 68, pp. 537-566.

Lee, W.G. and Chung, M.K., 1995, "The Equilibrium States and the Stability Analysis of Reynolds Stress Equations for Homogeneous Turbulent Shear Flows," *Phys. Fluids*, Vol. 7, pp. 2807-2819.

Liljegren, L.M., 1993, "The Effect of a Mean Fluid Velocity Gradient on the Streamwise Velocity Variance of a Particle Suspended in a Turbulent Flow," *Int. J. Multiphase Flow*, Vol. 19, pp. 472-484.

Rahshaida, A.A., 1999, "A Computational Model for Predicting Particle Transport in Turbulent Flows," M.Sc. Thesis, University of Saskatchewan, Saskatoon, SK.

Rogers, M.M. and Moin, P., 1987, "The Structure of the Vorticity Field in Homogeneous Turbulent Flows," *J. Fluid Mechanics*, Vol. 176, pp. 33-66.

Stock, D.E., 1996, "Particle Dispersion of Flowing Gases - 1994 Freeman Scholar Lecture," *ASME J. Fluids Engineering*, Vol. 118, pp. 4-17.

Taulbee, D.B., Mashayek, F., Givi, P., and Barre, C., 1997, "Simulation and Reynolds Stress Modeling of Particle-Laden Turbulent Shear Flows," *Proc. 11th Symp. Turbulent Shear Flows*, 24:17-24:22.

Tavoularis, S. and Corrsin, S., 1981, "Experiments in Nearly Homogeneous Turbulent Shear Flow with a Uniform Mean Temperature Gradient. Part 1," *J. Fluid Mechanics*, Vol. 104, pp. 311-347.

Tavoularis, S., 1985, "Asymptotic Laws for Transversely Homogeneous Turbulent Shear Flows," *Phys. Fluids*, Vol. 28, pp.999-1001.

Yeh, F. and Lei, U., 1991, "On the Motion of Small Particles in a Homogeneous Turbulent Shear Flow," *Phys. Fluids A*, Vol. 3, pp. 2758-2776.

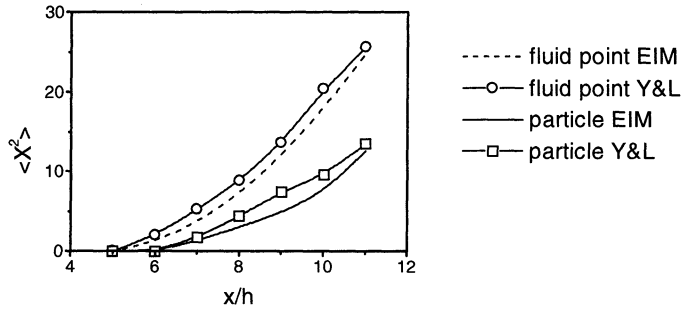

Figure 1a. Streamwise dispersion rate for zero drift velocity, $d_p = 57\mu m$.

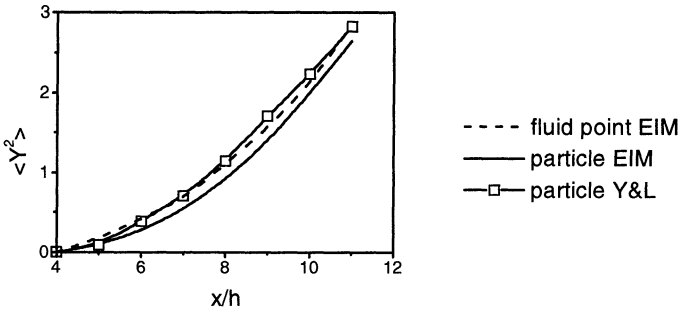

Figure 1b. Transverse dispersion rate for zero drift velocity, $d_p = 57\mu m$.

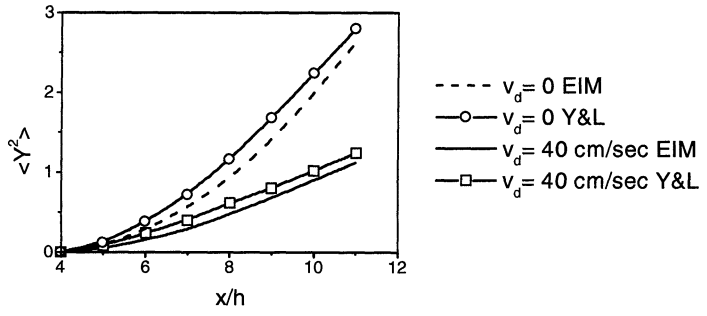

Figure 2. Transverse dispersion rate for finite drift velocity, $d_p = 57\mu m$.